EVALUATING THE LOCAL STRENGH AND CRACK RESISTANCE OF AN GLASS FIBER EPOXY COMPOSITE IN THE INTERLAYER TENSION AND SHEAR USING A FINITE-ELEMENT MODEL AND EXPERIMENTALLY DETERMINED PARAMETERS OF THE COHESIVE ZONE

P. G. Babaevsky,[1]* N. V. Salienko,[1] and A. A. Shatalin[2]

A systematic evaluation of the interlayer crack resistance in the modes I and II loadings of a glass fiber epoxy laminated composite by experimental and computational methods using the cohesive zone model was carried out. The local properties (the ultimate stress σ_C, the maximum displacement $\delta_{\max}$, and the specific work of fracture γ_F) of the cohesive zone were determined experimentally by the methods of separation and shear of the layer contact zone; the critical intensities of elastic energy release (G_{IC} and G_{IIC}) were found by the method of linear elastic fracture mechanics. Based on the experimental data obtained, the critical length of the cohesive zone was calculated by the Barenblatt micromechanical theory. A numerical evaluation of the crack resistance of a laminated composite under conditions of static loading in the modes I and II was carried out using 3D finite-element models of a double-cantilever beam and end-notched flexure specimens with an implemented cohesive zone obeying the exponential law. The optimal number of interface elements in the finite-element mesh was determined for the cohesive zone calculated based on experimental data, which ensured a sufficient accuracy of numerical calculating the ultimate load of the onset of crack growth and the stress distribution along the length of the cohesive zone with a minimum number of calculations. The approach proposed and the results obtained showed a good agreement between the calculated and experimentally determined characteristics of standard specimens of glass fiber epoxy composite and can be used to calculate the interlayer strength and crack resistance of structural members with a complex geometry made of layered polymer composites.

[1]Moscow Aviation Institute, Moscow, 125993 Russia
[2]Joint-Stock Company "NIIgrafit", Moscow, 111524 Russia
*Corresponding author; e-mail: pgbabayevs@mail.ru

1. Introduction

Laminated glass fiber composites based on rigid polymer matrices and fiberglass fabrics or nonwoven fibrous components, like other layer-reinforced polymer composite materials (PCMs), are widely used to create the lightweight load-bearing structures and their members [1, 2]. Layered PCMs have obvious advantages over the traditional types of structural materials in terms of specific stiffness and strength, with wide technological possibilities for a directed control of their structure and properties in the plane of layers. The main disadvantage of such PCMs is their low resistance to an origination and evolution of defects/cracks between layers under the action of residual stresses, external loads, and environmental factors during the production process and operation of the structures. Therefore, the estimation and prediction of the interlayer strength and crack resistance of layered PCMs is currently one of the most important tasks in the design and production of structural members from them [3-8].

To characterize the conditions for the initiation and growth of interlayer defects/cracks in pseudo-brittle layered PCMs, it is widely used the energy parameter of load on a crack (the crack driving force, CDF), introduced in the linear elastic fracture mechanics (LEFM). This is the so-called intensity of the elastic energy release G accumulated during deformation per unit area of the surface formed during the growth of a defect/crack in three simple loading modes, namely, tension (G_I), shear (G_{II}), and antishear (G_{III}) [9]. In this case, a simple failure criterion (the initiation of defect/crack growth) under a given loading mode in the LEFM is the achievement of the critical value G_C ($G \geq G_C$) of CDF, which is a material property called as the crack resistance (CR) parameter. For a nonbrittle fracture, the equivalent parameters of CDF and CR are the path-independent integral J and its critical value J_C, respectively.

The analytical methods of LEFM make it possible to calculate the parameters of CDF, and experimental methods enable to determine their critical values, i.e., CR parameters for three loading modes and their combinations (mixed modes) using simple standard specimens with a crack of given type, i.e., to solve the primary problem of a multilevel pyramid of computational and experimental evaluation and prediction of the strength and load-bearing capacity of structural members made of layered PCMs in terms of their resistance to delamination [9-13]. Both analytical and experimental evaluations of these parameters are difficult or impossible for layered PCMs with a complex geometry and in a combined stress state when solving problems of higher levels of this pyramid.

To solve these problems, in the past two decades, within the framework of LEFM, using the finite-element method (FEM), numerical methods for estimating the conditions of propagation of interlayer cracks in layered PCMs and adhesive joints close to them were developed intensively. To date, the two main methods implemented in the FEM for estimating the CDF and CR have obtained the greatest development, namely, the virtual crack closure method (FEM/VCCM) [14, 15] and the cohesive zone method (FEM/CZM) [16-25].

In the FEM/VCCM, using the finite element ABAQUS or ANSYS software, calculation of the intensity of elastic energy release is based on the results of 2D (continuous) or 3D (solid-state) one- or two-step finite-element analysis methods, which allow one to realize the separation by loading modes. In this method, the singular stress field at the front (tip) of the crack is calculated using specially developed finite elements, whose vibration behavior depends on their size and can lead to a computational instability. Numerical experiments have shown that for layered PCMs, the selection of length of the initial crack has a small effect on the accuracy and complexity of calculations [21] when choosing the size of such elements between ½ and ¼ of a layer thickness.

Based on the calculated CDF (G) and the CR parameters known for three separate or mixed loading modes ($G_C = 2\gamma F$), a failure criterion is selected in relation to the parameters of the CDF/CR as the degree of damage. The equality of this ratio to unity corresponds to the failure condition, i.e., the onset and growth of an interlayer defect/crack. When using the VCCM, the main problems within the framework of LEFM are caused by the fact that a crack has to be developed a self-similarly, i.e., the shape of its front has to be not change during germination, which is often not the case, and also by the fact that initial crack has to be a finite length, since the calculated CDF tends to zero when the crack length tends to zero. However, the policy of "zero intolerance to the growth of defects/cracks" in the certification of the members of aircraft

structures made of laminated reinforced PCMs allows the application of these methods to numerical estimation and prediction of the strength and load-bearing capacity of such structures [7, 8].

The second main method of numerical estimation of the conditions of interlayer crack growth in layered PCMs (FEM/CZM) is the use a more physically based approach based on the implementation of the cohesive zone model into the FEM model. This method, first proposed in [16] for concrete, is based on the Barenblatt micromechanical model [24] developed within the framework of LEFM, in which the crack growth conditions are determined by the development of local prefracture processes and, accordingly, by the local deformation-strength properties of the material at the crack tip.

In the 3D FEM/CZM, when using the ABAQUS or ANSYS software, the cohesive zone (CZ) is defined as an area of zero thickness with a separate mesh from special interface finite elements (IFEs) connecting two solid sides of the crack. In numerical calculations, the force causing the displacement of crack sides ($P - \Delta$) in a given loading mode is estimated using four main short circuit parameters (CP): pseudo-stiffness K, the maximum stress σ_C, the limit displacement $\delta_{\max}$, and the specific work of destruction ($2\gamma F = G_C = \sigma_C \delta_{\max}$), corresponding to the law of the cohesive zone (CZL). In accordance with micromechanical concepts, all these parameters characterize the local deformation-strength properties of the material at the tip of the crack.

An important problem of numerical calculations using the FEM/CZM is the strong dependence of the accuracy and complexity (duration and volume) of calculations on the size of IFE mesh cells. With increasing their length, i.e., decreasing their number, the volume and the accuracy of calculations both decrease. On the contrary, with increasing the number of IFEs above a certain value, the accuracy of calculations increases, but, at the same time, their laboriousness increases much more sharply, as wells as the convergence of results, i.e., computational stability, may be lost [26].

The high complexity of numerical calculations in the FEM/CZM, while ensuring a sufficient accuracy of calculations, makes difficult to use it in practice for estimating and predicting the strength and load-bearing capacity of rather complex structural members made of layered reinforced PCMs in terms of their CR parameters. It is obvious that the optimization of the length and number of IFEs to ensure a sufficient accuracy and minimization the complexity of calculations can be achieved by setting the IFEs for a specific material using experimentally determined CZL parameters on simple (standard) specimens and given loading modes with their further use in calculating more complex specimens or structural members [19-23, 25].

The objective of this paper was to check the possibility of choosing optimal dimensions of the finite-element mesh on the example of model specimens of a layered glass fiber epoxy composite and, accordingly, the number of IFEs located along the cohesive zone which would provide a sufficient accuracy of numerical calculations of crack growth conditions with a minimum computational complexity using experimental data and methods for determining the parameters of local deformation-strength properties of layered PCMs corresponding to the CZL during the development of interlayer defects/cracks in the modes I and II.

2. Experimental Evaluation of the CZL and CR Parameters of a Layered Glass Fiber Epoxy Composite under Tension and Shear

The object of the study was thin plates of a layered orthotropic glass fiber epoxy composite (GFEC) produced by vacuum molding from a prepreg based on a T-10 satin fiberglass fabric [31] and a model epoxy binder prepared with an equimolar mixture of ED-20 epoxy resin and a diaminodiphenylmethane hardener. The technological package was formed on the working surface of a flat metal plate with an antiadhesive polyimide film by layer-by-layer stacking of the prepreg. For the primary sealing of layers and the removal of air from the bag, an vacuumed bag made of a nylon film was used. The final molding of the plates and curing of the binder were carried out in a vacuum oven at a residual pressure of not more than 0.8 kgf/cm² and heating rate of 2°C/min to 125 ± 5°C, holding at this temperature for 1 h, followed by heating to 180 ± 5°C with an exposure for 5 h and cooling to room temperature at a rate of about 1°C/min. Specimens of
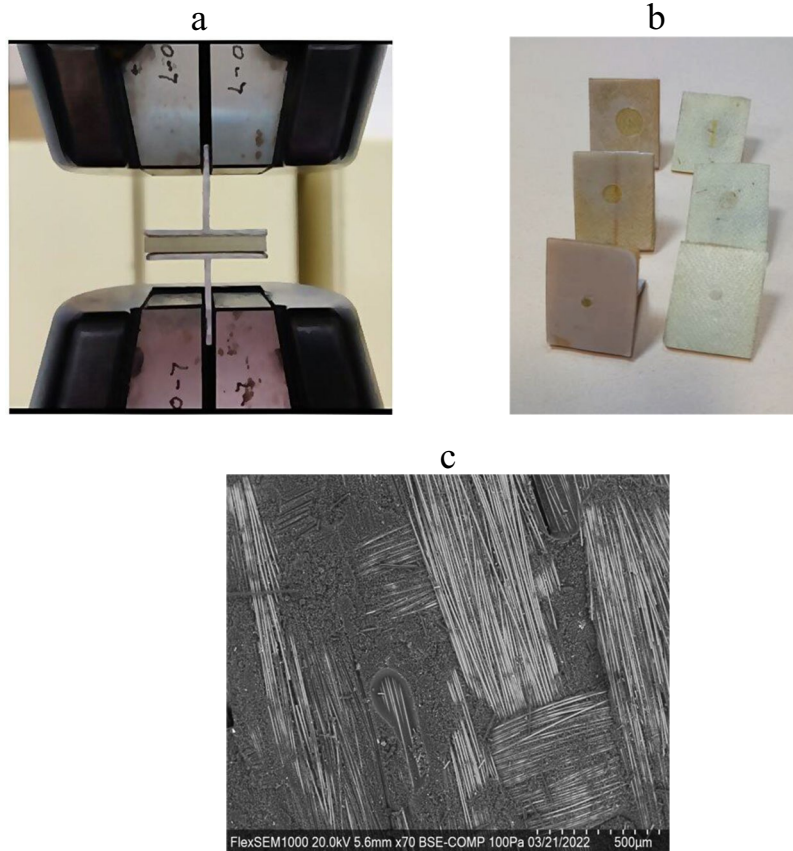
Fig. 1. (a) GFEC specimen for evaluating the interlayer deformation-strength properties at local separation in jaws of a tensile testing machine, (b) optical photographs of the surface of specimens with contact zones of 3, 6, and 10-mm in diameter after destruction, and (c) scanning electron micrograph of the fracture surface.

the required dimensions were mechanically cut from the plates. The ratio of glass fibers and polymer matrix in the GFEC after molding was 67:33 (wt%).

The local interlayer deformation-strength properties of the GFEC as the parameters of the CZL under loading modes I and II (ultimate stresses σ_{IC} and σ_{IIC}, and ultimate strains $\delta_{I\max}$ and $\delta_{II\max}$ during separation and shear, respectively), were determined using non-standard methods.

The specimens for separation tests were prepared from 50×40×3-mm plates molded from 14 prepreg layers. During formation of the technological package, between the 7th and 8th layers of the prepreg, a fluoroplastic film 10-μm thickness was laid, in the center of which the round holes of 10, 6, and 3 mm in diameter were cut to form a local interlayer contact (imitation of the cohesive zone). Specimens of 30×25 mm in size were cut out from the central part of molded plates. Aluminum corners were glued with a VK-27 glue to the specimens to help their fixation in the grips of the tensile testing machine (Fig. 1a).

For the local interlayer shear test, the specimens were made according to the method elaborated by Yu. M. Tarnopolsky and T. Ya. Kintsis [27]. The specimens were cut from GFEC plates of 220×150×3 mm in size, molded in the same way as in the case of the specimens for the local separation test. During formation of the technological package, in its middle part along the entire length of the plate, a strip of a fluoroplastic film of 10-μm thickness and 15-mm width was laid, in which round holes with a diameter of 10, 6, and 3 mm were cut out at a given distance to form a local interlayer
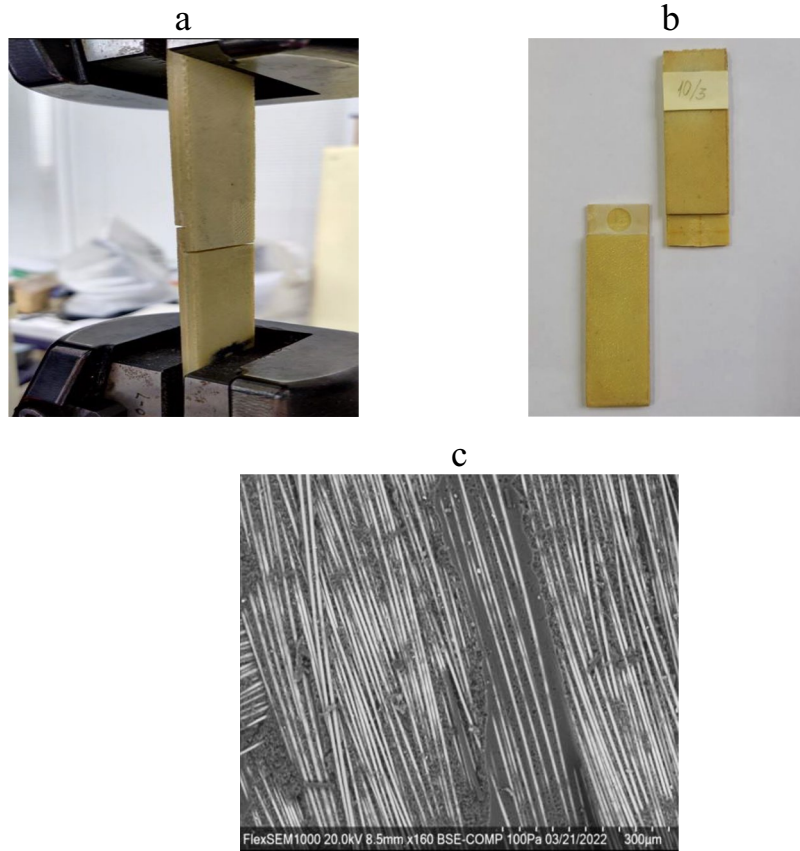
Fig. 2. (a) GFEC specimen for evaluating the local interlayer deformation-strength properties under shear in grips of a tensile testing machine, (b) optical photograph of the specimen surface after fracture, and (c) scanning electron micrograph of the delamination surface.

contact (imitation of the cohesive zone). From the molded plates, test specimens with a size of 200×20×3 mm were cut, in whose center there was the contact zone. Using a diamond wheel, one notch was made to the depth of film placement the from the top and bottom surfaces of specimens in the vertical (transverse) plane, so that only the contact zone was shifted during tension.

The specimens were tested under laboratory conditions at a normal temperature and normal relative humidity. Five specimens with three interlayer contact sizes were tested for separation and shear at a traverse displacement speed of the tensile testing machine equal to 2 mm/min. The force F was recorded by a dynamometer; the absolute displacement of the cohesive zone δ was measured by an LVDP TRS-0025 sensor with an accuracy 0.075%. To avoid the occurrence of shear stresses and to ensure a uniform normal separation of the layer adhesion zone, the specimens of the first type were carefully balanced in a horizontal plane. During mode II shear tests, the specimen was carefully aligned in the horizontal and vertical planes to avoid the appearance of bending moments.

The electron micrographs of fracture surfaces of the local adhesion zones of glass fiber epoxy composite layers are shown in Figs. 1c and 2c. It is seen that the failure of layers during the separation and shear tests was mainly associated with the matrix failure and its adhesive separation from the fiberglass fabric. When tested for the interlayer separation, a certain amount of broken fibers was observed, which was not present during shear tests. Thus, the local failure of GFEC under the action of tensile and shear loads had a mixed adhesive-cohesive character with an insignificant proportion of broken (bridging) fibers during tests in mode I.
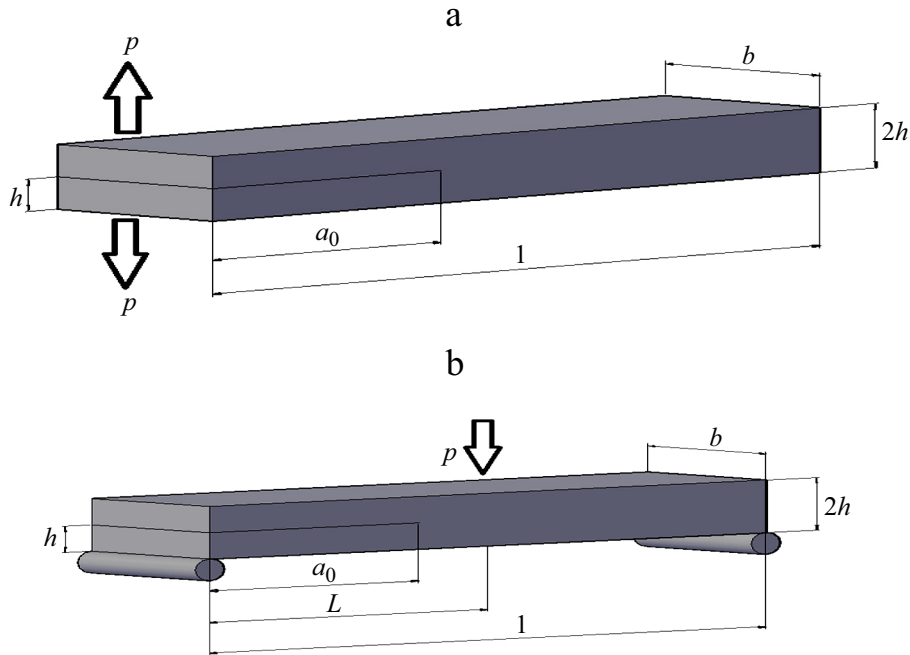
Fig. 3. General view, dimensions, and loading scheme of DCB (a) and ENF (b) specimens: $l = 150$ mm, $b = 20$ mm, $h = 2$ mm, and $a_0 = 45$ mm.

TABLE 1. Values of Local Properties of the Contact Zone of GFEC of Various Sizes in Loading Modes I and II

Contact zone diameter, m	Loading mode: I/II			
	σ_C, MPa	δ_{max}, μm	γF, J/m²	G_C, local J/m²
10	9.2/12.8	45/51	207/326	414/652
6	10.5/14.6	40/47	210/343	420/686
3	13.5/17.3	34/42	230/363	460/726

The ultimate local stresses at separation (σ_{IC}) and shear (σ_{IIC}) tests were determined from the ratio of the separation (F_I) and shear (F_{II}) forces to the area s of the fracture zone. The area under the $\sigma_I - \delta_I$ and $\sigma_{II} - \delta_{II}$ curves corresponds to the specific work of formation of a new surface γF upon the contact zone failure.

According to the Barenblatt micromechanical model developed within the LEFM framework, the energy parameter of crack resistance, as the critical value of intensity of the elastic energy release during crack growth, is $G_C = \sigma_C \delta_{max}$, i.e., double the area under the curves $\sigma - \delta$ as the specific work of the local zone failure at the crack tip: $G_C = 2\gamma F$. It follows from here that the limiting values of the parameters of crack resistance of the layered glass fiber composite calculated by the micromechanical model and local experimental data were $G_{IC} = 460$ J/m², and in shear $G_{IIC} = 726$ J/m².

The local properties of GFEC contact zone calculated from experimental data in the normal separation and shear are summarized in Table 1.

To directly determine the global values of G_{IC} and G_{IIC} of GFEC by the experimental LEFM, the DCB (double cantilever beam) specimens with an edge crack were loaded in to mode I according to GOST 56815-2015 [28] and ENF (end-node flexure) specimens with an edge crack were loaded in mode II according to GOST 33685-2015 [29]. Specimens (Fig. 3) with a predetermined interlayer crack were cut out from plates of 170×40×4 mm size, produced by laying 20

prepreg layers and molding according to the method and regimes described above. In the process of layup, a fluoroplastic film of 10-µm thickness and 65-mm width was laid from one edge of the layups (between 10th and 11th layers) in a horizontal plane across the longitudinal axis, to form the initial crack.

The general view, dimensions, and loading scheme of the specimens are shown in Fig. 3.

T-shaped aluminum profiles were glued to the surfaces of DCB specimens at the crack edge by a VK-27 glue to fix them in grips of the testing machine and open the crack beyond the edges of the specimens. The ENF specimens were tested at three-point bending in a special device.

Before testing, the end of the defect created by the fluoroplastic film was finished with a sharp blade, and the initial length of the crack was visually recorded. Tests in tension and bending were carried out under normal conditions at a speed of 2 mm/min, recording the load, displacement, and length of the crack.

The critical intensity of the elastic energy release in loading mode I (G_{IC}) was calculated from the maximum load P_C corresponding to the beginning of critical propagation of the crack by the formula [28]

$$G_{IC} = \frac{4P_C^2}{E_f b^2}\left(\frac{3a^2}{h^3} + \frac{1}{h}\right),$$ (1)

where E_f is the elastic modulus in transverse bending of the layered GFEC, h is the specimen half-thickness, b is its width, and a is length of the edge crack.

The critical value of G_{IIC} in the mode II loading was also calculated from the maximum load P_C corresponding to the beginning of critical propagation of the crack and the beam deflection δ by the formula [29, 30]

$$G_{IIC} = \frac{9a^2 P_C \delta}{2b\left(2L^3 + 3a^3\right)},$$ (2)

where L is half the distance between supports.

The average global values of G_C obtained for the specimens in loading modes I and II were 468 and 732 J/m², respectively.

2. Finite-Element Analysis of the Crack Resistance of Specimens of Layered Glass Fiber Epoxy Composites of the DCB and ENF Types Using Experimental Data

The numerical simulation of the crack growth process in specimens of DCB and ENF types was carried out using the ANSYS Mechanical APDL software. The virtual delamination of specimens in modes I and II was carried out by 3D finite-element models with dimensions of physical specimens (see Fig. 3), and a given initial crack length of 45 mm. The geometric models of the specimens contained two types of finite elements: solid-state Solid 185 and interface Inter 205. These elements are available in the finite-element library of the software package. The semi-beams of geometric models were divided by a regular mesh of Solid 185 finite elements. The elastic characteristics of the orthotropic GFEC [6, 14] were as follows: Young's moduli $E_{11} = 20$ GPa, $E_{22} = 18$ GPa, and $E_{33} = 3.5$ GPa, Poisson's ratios $v_{12} = 0.24$, $v_{13} = 0.24$, and $v_{23} = 0.45$, and shear moduli ($G_{23} = 4.2$ GPa, $G_{12} = 4.2$ GPa, and $G_{13} = 3.18$ GPa.

The zero-thickness IFEs were located along the half-beam contact boundary in the virtual specimens; they tied the potential crack edges together until the crack began to grow. To numerical evaluation of the interlayer delamination resistance, a bilinear CZL with experimentally determined CZ parameters for the virtual specimens was set in the command line of the program interface for Inter 205 elements:

the maximum adhesion strength σ_{IC} ($C_1 = 13.5$ MPa) and the maximum opening $\delta_{I\max}$ ($C_2 = 0.034$ mm) for DCB specimens;

the maximum delamination shear stress σ_{IIC} ($C_3 = 17.3$ MPa) and the maximum shear strain $\delta_{II\max}$ ($C_4 = 0.042$ mm) for ENF specimens.
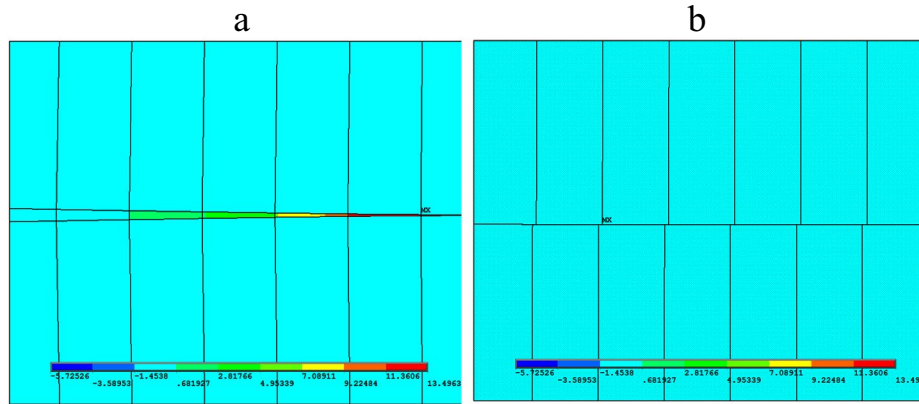
Fig. 4. Examples of visual images of the distribution of local stresses along the length of a numerical CZ for a given length of the IFE in virtual specimens of DCB (a) and ENF (b).

The interaction between the internal surfaces of the model and the adhesion zone between them was set using software tools; and a regular IFE mesh of a given length was formed along the whole path of the crack growth expected.

To select optimal dimensions of the finite-element mesh, i.e., the length l_e and number N_e of IFEs located along the CZ length and providing a sufficient accuracy of numerical calculations of crack growth conditions with a minimal computational complexity, we used the CZ length l_{CZ} equal to that calculated from experimentally determined parameters of the layered GFEC using the equation [24]

$$l_{CZ} = \frac{\pi}{8} \frac{MG_C}{\sigma_C^2}$$ (3)

of the micromechanical Barenblatt model, where M is the transverse Young's modulus (E_{33} =3.5 GPa) and shear modulus (G_{13} = 3.18 GPa); G_C and σ_C are the interlayer local CZ parameters given in Table 1 for loading mode I (G_{IC} =460 J/m^2; σ_{IC} = 13.5 MPa) and mode II (G_{IIC} = 726 J/m^2; σ_{IIC} = 17.3 MPa). The calculated values of l_{CZ} for these loading modes were 3.52 and 3.36 mm, respectively. For investigation, we chose lengths l_e equal to 2, 0.9, 0.5, and 0.1 mm. The number N_e of l_e located along the length of CZ was calculated by the formula:

$$N_e = \frac{l_{CZ}}{l_e}$$ (4)

with rounding of fractional values. For the virtual specimens of DCB and ENF types with l_e = 2 mm (N_e = 1.76 and 1.68), two elements were used in the simulation with l_e = 0.9 mm (N_e = 3.91 and 3.73), four elements with l_e = 0.5 mm (N_e = 7.04 and 6.72), seven elements with l_e = 0.1 mm (N_e = 35.2 and 33.6), 35 and 34 elements, respectively.

After setting the number of l_e in the finite-element analysis of the development of CZ, a load was applied, the degrees of freedom along the model boundaries were restricted, and the calculation parameters were adjusted in the program processor. In the simulation, a virtual crack growth generated. Calculation results were analyzed in the post-processor of the software package. They automatically displayed as visual images of local stresses in the CZ on the IFE mesh during the crack growth at the virtual delamination of DCB and ENF specimens and graphical relations of their distribution along the CZ length from the crack tip, as well as of graphical relations of the global load on crack edges on the opening or displacement of its edges in modes I and II, respectively, characterizing the resistance of specimens to the crack initiation and growth.
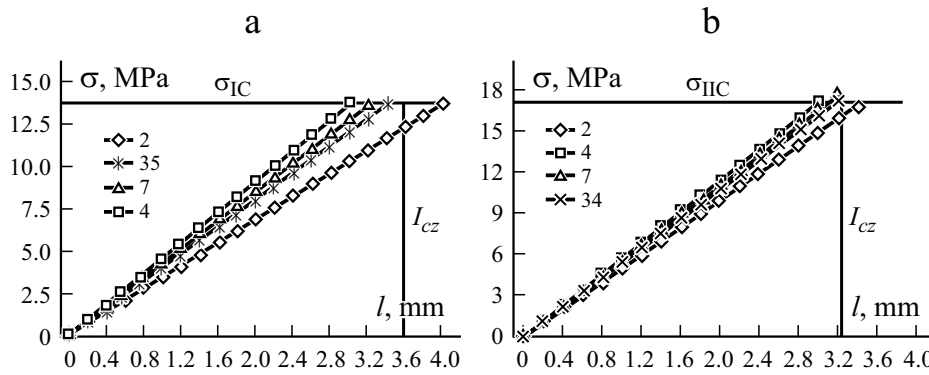
Fig. 5. Distributions of local stresses along the length of the numerical CZ (by distance from the crack tip) for different lengths of IFE in virtual DCB (a) and ENF (b) specimens.
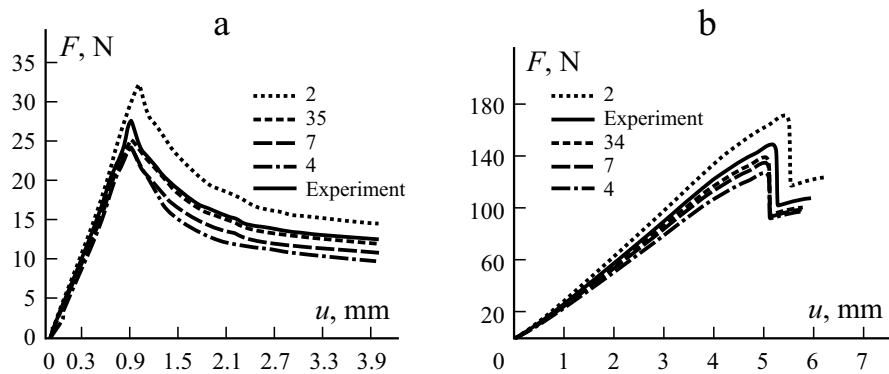

Fig. 6. Calculated (at different amounts of IFEs) and experimental relations of the load vs. displacement of crack edges for DCB (a) and ENF (b) specimens.

Figure 4 demostrates the examples of visual images of the distribution of local stresses along the length of a numerical CZ for a given length IFE. Figure 5 shows the graphical dependences of their distribution along the CZ length from the crack tip for different numbers of IFEs.

The horizontal and vertical thin lines in Fig. 5 correspond to experimentally determined parameters of the local interlayer strength of the GFEC (σ_{IC} and σ_{IIC}) and the cohesive zone length calculated from the experimental data (l_{CZ}) for various loading modes. The proximity of intersection of these lines to the intersection with them of the calculated relations of the local stress depending on a distance from the crack tip characterizes the calculation accuracy in comparison with the experimental data.

Figure 6 shows the graphical relations between the load on crack edges and the opening or displacement of its edges in modes I and II, respectively, calculated at different numbers of IFEs and experimentally obtained testing the GFEC specimens on global crack resistance, whose peak values characterize the resistance of specimens to the initiation and growth of cracks.

The closeness of the calculated curves to the experimental ones also serves as a characteristic of calculation accuracy. Table 2 shows the calculated and experimental values of global G_C obtained for loading modes I and II.

The data presented in Figs. 5 and 6 and Table 2 for both types of loads and both types of calculations show that, in the numerical estimation of the crack resistance of specimens, a sufficient approximation to experimental data was observed

TABLE 2. Calculated and Experimental Values of Global G_C Determined in Loading Modes I and II

G_C value	Number of IFEs along the CZ length	G_{IC}, J/m²	G_{IIC}, J/m²	Discrepancy with $G_{C\exp}$ (mode I/ mode II), %
Experimental	–	468	732	–
	2	538	854	14.9/16.6
	4	432	667	7.7/8.9
Calculated	7	436	676	6.8/7.6
	34	–	692	–/5.5
	35	446	–	4.7/–

when the number of IFEs per CZ was at least four. An increase in the number of IFEs per CZ length led to an increased calculation accuracy, whereas the volume and duration of calculations increased sharply.

Conclusion

The results obtained in this work and their analysis show that experimental and numerical methods for estimating the interlayer crack resistance of layered PCMs in the form of simple standard DCB and ENF specimens, including the experimental determination of the parameters of local interlayer deformation-strength properties of the material and numerical simulation by the finite-element method of the stress-strain state of a given specimen with a cohesive zone implemented at the place of stress concentration or an existing interlayer defect (crack) with a known law and loading mode, can serve as the basis for the development of effective numerical methods for calculating the interlayer strength and crack resistance of complex structurally similar specimens, structural members, and structures made of layered PCMs. On the other hand, such techniques can be effective in solving material science and technological problems in developing the composition, structure, and production methods, and molding regimes of layered PCMs with an increased interlayer crack resistance.

REFERENCES

1. A. I. Preobrazhensky, "Glass-fiber-reinforced plastics: properties, technologies, and application," Glavnyi Mekhanik, No. 5, 27-36 (2010).
2. T. P. Sathishkumar, S. Satheeshkumar, and J. Naveen, "Fiberglass-reinforced polymer composites — a review," J. Reinf. Plastics and Compos., **33**, No. 13, 1258-1275 (2014).
3. A. N. Vorontsov, G. Kh. Murzakhanov, and V. N. Shchugorov, "Delamination failure of composite structure," Mech. Compos. Mater., **6**, 1007-1023 (1989).
4. H. B. Kahla, Z. Ayadi, and J. Varna, "Local delaminations induced by interaction between intralaminar cracking and specimen edge in quasi-isotropic CF/EP NCF composites in fatigue loadings," Mech. Compos. Mater., **56**, No. 3, 291-302 (2020).
5. V. E. Strizhius, "A methodology for estimating the delamination growth rate in layered composites under tensile cyclic loading," Mech. Compos. Mater., **56**, No. 4, 533-540 (2020).
6. L. Wang, C. Zheng, H. Luo, S. Wei, and Z. Wei, "Continuum damage modeling and progressive failure analysis of carbon fiber/epoxy composite pressure vessel," Heavy Castings and Forgings, 475-480 (2015).

7. T. K. O'Brien, "Development of a composite delamination fatigue life prediction methodology," NASA Technical Reports Server, 1-9 (2009).

8. J. Bertolini, B. Castanié, J. J. Barrau, and J. P. Navarro, "Multi-level experimental and numerical analysis of composite stiffener debonding," Part 1, Nonspecific Specimen Level, Composite Structures, **90**, 381-391 (2009); Part 2, Element and Panel Level, Compos. Struct., **90**, 392-403 (2009).

9. P. Babaevsky and S. Kulik, Crack Resistance of Cured Polymer Compositions [in Russian], Khimiya, Moscow (1991).

10. A. J. Brunner, B. R. K. Blackman, and P. Davies, "A status report on delamination resistance testing of polymer matrix composites," Eng. Fracture Mech., **75**, 2779-2794 (2008).

11. V. M. Mirsalimov, "Modeling the initiation and propagation of cracks in a fibrous composite under loading across fibers," Mech. Compos. Mater., **56**, No. 6, 721-734 (2021).

12. V. D. Krylov, N. O. Yakovlev, Yu. A. Kurganova, and O. A. Lashov, "Interlayer crack resistance of structural polymer composite materials," Aviats. Mater.Tekhnologii, **40**, No. 1, 79-85 (2016).

13. N. Trivedi, S. Das, and E.-M. Craciun, "The mathematical study of an edge crack in two different specified models under time-harmonic wave disturbance," Mech. Compos. Mater., **58**, No. 1, 1-14 (2022).

14. R. Krueger, "Virtual crack closure technique: History, approach, and applications," Appl. Mech. Rev., **57**, No. 2, (2004).

15. E. Pietropaoli, "Virtual crack closure technique and finite-element method for predicting the delamination grows initiation in composite structures," Intechopen.com (2008).

16. A. Hillerborg, M. Modéer, and P. Petersson, "Analysis of crack formation and crack growth in concrete by means of fracture mechanics and finite elements," Cement Concrete Res., **6**, No. 6, 773 (1976).

17. G. Alfano and M. Crisfield, "Finite-element interface models for the delamination analysis of laminated composites: mechanical and computational issues," Int. J. Numerical Methods in Eng., **50**, No. 7, 1701-1736 (2001).

18. A. Turon, C. G. Dávila, P. P. Camanho, and J. Costa, "An Engineering solution for using coarse meshes in the simulation of delamination with cohesive zone models," NASA/TM, 213547 (2005).

19. P. Harper and S. Hallett, "Cohesive zone length in numerical simulations of composite delamination," Eng. Fract. Mech., **75**, No. 16, 4774-4792 (2008).

20. P. Harper and S. R. Hallett, "A fatigue degradation law for cohesive interface elements — Development and application for composite materials," Int. J. Fatigue, **32**, 1774-1787 (2010).

21. B. Cox and Q. Yang, "Cohesive models for damage evolution in laminated composites," Int. J. Fract., 107-137 (2005).

22. Moslemi M., Khoshravan M. Cohesive zone parameters selection for mode I prediction of interfacial delamination," J. Mech. Eng., **61**, No. 9, 507 (2015).

23. P. G. Babayevsky, N. V. Salienko, and G. V. Novikov, "Use of experimentally determined parameters of the cohesive zone in the numerical evaluation of the resistance to delamination of polymer composites materials," Inorg. Mater. Appl. Res., **10**, No. 5, 1259 (2019).

24. G. I. Barenblatt, "The mathematical theory of equilibrium cracks in brittle fracture," Adv. Appl. Mech.,**7**, 55 (1962)

25. Z. Z. Wang, J. Zhao, X. Ma, S. J. Wang, and X. Yang, "Numerical simulation of progressive delamination in composite laminates under mode I and mode II loadings," Mech. Compos. Mater., **56**, No. 6, 735-746 (2021).

26. S. Masooda, A. Singh, and S. Viswamurthy, "Simulation & validation of delamination growth in CFRP specimens under mixed mode loading using cohesive elements," Proceedings of 14th ISAMPE National Conference on Composites (INCCOM-14), Hyderabad (2016).

27. GOST 19170-2001. Fiberglass. Construction fabric. Specifications, Standards Publishing House, Minsk.

28. Yu. M. Tarnopolsky and T. Ya. Kintsis, Methods of Static Testing of Reinforced Plastics [in Russian], Khimiya, Moscow (1981).

29. Standard 56815-2015. Polymer composites. Method for determination of the specific work of exfoliation in tearing off conditions G_{IC}, Standardinform, Moscow.

30. Standard 33685-2015. polymer composites. Test method for determination of the interlaminar fracture toughness under shear G_{IIC}, Standardinform, Moscow.

31. M. Moslemi and M. K. Azar, "Delamination analysis of woven fabrication laminates using cohesive zone model," J. Cent. South Univ., **23**, 27-38 (2016).

32. GOST 56805-2015. Polymer composites. Methods for determining mechanical characteristics in bending, Standartinform, Moscow.